"TITU MAIORESCU" UNIVERSITY BUCHAREST
FACULTY OF DENTAL MEDICINE
DOCTORAL SCHOOL

DOCTORAL THESIS
ABSTRACT

NANOSTRUCTURED MATERIALS FOR DENTAL APPLICATIONS

Scientific Supervisor:
Prof. Univ. Dr. Cornelia BÎCLEŞANU

PhD Candidate:
Ana Maria Gianina REHNER (COSTACHE)

TABLE OF CONTENTS

LIST OF PUBLICATIONS

1. Rehner, A.M.G.; Bratu, A.G.; Bîrcă, A.C.; Niculescu, A.-G.; Holban, A.M.; Hudiță, A.; Bîclesanu, F.C.; Balaure, P.C.; Pangică, A.M.; Grumezescu, A.M.; et al. Zn_2SnO_4@SiO_2@5-FU Nanoparticles as an Additive for Maxillary Bone Defects. *Int. J. Mol. Sci.* **2025**, *26*, 194. https://doi.org/10.3390/ijms26010194, **Factor de impac 4.9**.
2. Rehner, A.M.G.; Tudorache, D.-I.; Bîrcă, A.C.; Nicoară, A.I.; Niculescu, A.-G.; Holban, A.M.; Hudiță, A.; Bîclesanu, F.C.; Balaure, P.C.; Pangică, A.M.; et al. Antibacterial Properties of PMMA/ZnO(NanoAg) Coatings for Dental Implant Abutments. *Materials* **2025**, *18*, 382. https://doi.org/10.3390/ma18020382, **Factor de impac 3.1**.
3. Rehner, A.M.G.; Moldoveanu, E.T.; Niculescu, A.-G.; Bîclesanu, F.C.; Pangică, A.M.; Grumezescu, A.M.; Croitoru, G.A. Advances in Dental Implants: A Review of In Vitro and In Vivo Testing with Nanoparticle Coatings. *J. Comp. Sci.,* **2025**, in press.

Introduction

Nanotechnology (NT) has become a rapidly expanding research field, with significant applications in multiple domains, including dentistry. NT focuses on the design, fabrication, and characterization of materials, structures, and devices at the nanoscale, offering essential modifications to their physicochemical properties, such as improved mechanical strength, electrical conductivity, biocompatibility, and antimicrobial activity [1-5].

In dentistry, NT has opened new research directions and applications, ranging from early detection and diagnosis to innovative treatment options. Nanostructured materials (NM) are used for dentin remineralization, reduction of dental hypersensitivity, enhancement of adhesion in restorative materials, and protection against bacterial infections. A field of great interest is the use of nanoparticles (NP), which are integrated into dental composites to increase translucency, improve wear resistance, and inhibit bacterial biofilm formation [6-8]. Additionally, nanoparticles are used in dental coatings and sealants for disinfecting root canals, protecting exposed dentinal tubules, and reducing tooth sensitivity. Moreover, gold and silver nanoparticles are being investigated as radiosensitizing agents in oral cancer therapy, improving the efficacy of radiotherapy by enhancing the destruction of malignant cells [9,10].

Despite its benefits, NT raises concerns regarding potential side effects associated with the small size of nanoparticles, which can lead to their accumulation in organs, inflammation, and the risk of mutagenic effects. Furthermore, high production costs, lack of clear regulations, and limited knowledge about nanoparticle interactions with the human body present challenges that must be addressed through further research [11-16].

This research aims to develop and characterize innovative nanomaterials for bone regeneration and the protection of dental implants, addressing the need to overcome the limitations of conventional materials used in dentistry, such as insufficient implant integration, peri-implant infections, and poor bone regeneration. The proposed nanomaterials offer advanced solutions to optimize osseointegration, reduce the risk of post-implant infections, and improve the performance of restorative materials, while ensuring superior biological compatibility. This study fills a gap in the specialized literature by providing concrete data on the efficacy of nanomaterials in protecting dental implants and supporting bone regeneration.

By integrating multifunctional nanoparticles and exploring the applicability of nanotechnology in dentistry, this study makes a significant contribution to the development of advanced dental materials and opens new directions for more effective, safer, and personalized treatments. The results obtained have the potential to redefine standards in implantology and regenerative dental medicine, offering sustainable solutions for improving patients' quality of life.

The doctoral thesis is structured into two main sections: the literature review and the section dedicated to personal contributions, followed by general conclusions and highlights of the original aspects.

The literature review includes three chapters that provide a solid theoretical foundation for the conducted research: Chapter 1 presents the characteristics and synthesis methods of nanostructured materials, covering their classification and main synthesis techniques. Chapter 2 explores the applications of nanomaterials in dentistry, detailing their use in various fields, from orthodontic treatments to dental implantology and the diagnosis of oral diseases. Chapter 3 analyzes the safety, efficiency, and prospects of nanomaterials in dentistry, focusing on the prevention of post-implant infections, biocompatibility evaluation, and potential associated risks.

The personal contributions section consists of five chapters: Chapter 4 outlines the working hypotheses and general research objectives. Chapter 5 focuses on the statistical analysis of risk factors and post-operative complications associated with dental implants, offering a detailed perspective on clinical correlations. Chapters 6 and 7 are dedicated to experimental research: Chapter 6 addresses the development and characterization of Zn_2SnO_4@SiO_2@5-FU nanoparticles for bone regeneration and antimicrobial and antitumor therapy. Chapter 7 explores the synthesis and application of PMMA/ZnO(NanoAg)-based nanostructured coatings for the protection of dental implant abutments. Chapter 8 summarizes the general conclusions of the thesis, and Chapter 9 highlights the originality and innovative contributions of the research, emphasizing aspects that add value to the field of dentistry.

CHAPTER 4. WORKING HYPOTHESES AND GENERAL OBJECTIVES

The topic of this doctoral thesis, **"Nanostructured Materials for Dental Applications"**, is justified by the need to overcome the limitations of conventional materials used in dentistry. Modern dentistry faces significant challenges, such as peri-implant infections, insufficient bone tissue regeneration, and inadequate integration of filling materials or implants with host tissues. These issues, often associated with clinical failures, result in patient discomfort, post-operative complications, and additional costs for healthcare systems.

Nanotechnology offers an innovative approach to these challenges due to its ability to modify the physicochemical and biological properties of materials at the nanoscale.

The aim of this doctoral thesis is to develop and evaluate advanced nanomaterials, such as Zn_2SnO_4 coated with SiO_2 and functionalized with 5-Fluorouracil, alongside composites based on PMMA-ZnO/ZnO-Ag, for innovative applications in dentistry. Additionally, the study analyzes risk factors that may influence the success of dental implant treatments to implement individualized protocols.

The working hypothesis of this study was formulated based on theoretical and clinical premises suggesting that the success of dental implant treatments is influenced by several risk factors, including smoking, diabetes, hypertension, compliance with post-operative instructions, and the number of implants placed. It is hypothesized that optimal management of these factors can reduce the incidence of post-operative complications and improve the success rate of dental implants.

A statistical analysis was designed to test this hypothesis and determine the relationships between risk factors and the post-operative outcomes of patients. Using a rigorous quantitative approach, the study evaluated the distribution of risk factors, their correlations with observed complications, and the impact of each variable on implant success.

The study aimed to identify statistically significant associations that can guide clinical decisions and contribute to improving therapeutic protocols. The results obtained from the statistical analysis provide a clear perspective on how risk factors influence the success of implant treatments and suggest directions for optimizing post-operative management. These data can contribute to developing personalized prevention and treatment strategies, ensuring better patient monitoring and improving post-intervention quality of life.

Another working hypothesis of this research is based on the theory that using advanced nanomaterials, such as Zn_2SnO_4 nanoparticles coated with SiO_2 and functionalized with 5-Fluorouracil (5-FU), along with PMMA-ZnO/ZnO-Ag composite materials, can significantly enhance the performance of dental materials used in bone regeneration and implant protection. The

Zn_2SnO_4@SiO_2@5-FU nanoparticles are being investigated for their ability to support maxillary bone regeneration, while PMMA-ZnO/ZnO-Ag composites are analyzed for their potential to prevent biofilm formation on dental abutment surfaces.

These materials are considered capable of providing innovative solutions by combining antimicrobial, antitumor, and tissue-regenerating properties, ensuring increased biocompatibility and reducing the risks associated with peri-implant infections. In vitro studies will investigate the efficacy of nanomaterials in inhibiting the growth of pathogenic bacteria relevant to the oral cavity, as well as reducing the viability of tumor cells through mechanisms related to oxidative stress and direct interaction with cell membranes.

Assessing the biocompatibility of nanomaterials is a priority in this study. In vitro research will evaluate the interaction of these materials with human cells relevant to bone regeneration, testing their proliferation, viability, and differentiation in the presence of the studied nanoparticles. These tests will provide an in-depth understanding of the nanomaterials' potential to safely and effectively support tissue regeneration.

The general objectives of this study included: (i) Evaluation of the incidence of post-operative complications and the factors influencing them. (ii) Analysis of the relationship between smoking, diabetes, hypertension, and the success of dental implants.(iii) Investigation of the impact of compliance with post-operative instructions on reducing the risk of complications. (iv) Determination of the influence of the number of implants on post-operative outcomes and the need for medical follow-up. (v) Comparison of the results with existing data in the specialized literature to evaluate the consistency of the conclusions with previous studies.

Another objective is to assess the potential of Zn_2SnO_4@SiO_2@5-FU nanoparticles in supporting maxillary bone regeneration by examining their increased stability in solution, their capacity to inhibit Gram-positive bacteria, and their effectiveness in reducing cancer cell viability through oxidative stress mechanisms. Similarly, PMMA-ZnO/ZnO-Ag composite materials are evaluated for their ability to protect dental abutment surfaces against infections by reducing bacterial biofilm formation and promoting better interaction with peri-implant tissues.

The research focuses on the detailed characterization of the physicochemical and structural properties of the nanomaterials used. Zn_2SnO_4@SiO_2@5-FU and PMMA-ZnO/ZnO-Ag nanoparticles will be analyzed using advanced techniques, such as: X-Ray Diffraction (XRD), Scanning Electron Microscopy (SEM), Infrared Spectroscopy (IR).

These analyses aim to confirm the structure, composition, and stability of the developed materials.

This study places particular emphasis on optimizing the practical properties of nanomaterials for their use in dentistry. By addressing these innovations, the research seeks to develop materials capable of: Reducing the risks associated with peri-implant infections; Supporting complex tissue regeneration; Ensuring optimal integration with adjacent tissues.

The ultimate goal is to create a solid scientific foundation for introducing nanomaterials into modern dental practice, offering personalized and effective solutions to meet current clinical needs.

CHAPTER 5. STATISTICAL ANALYSIS OF RISK FACTORS AND POST-OPERATIVE COMPLICATIONS ASSOCIATED WITH DENTAL IMPLANTS

5.2. Materials and Methods

5.2.1. Description of the Patient Group and Inclusion/Exclusion Criteria

The study was conducted on a group of 250 patients who received dental implants over a defined period in a specialized dental unit. The selection of patients was based on strict inclusion and exclusion criteria aimed at ensuring the homogeneity of the sample and the relevance of the obtained results.

To be included in the study, patients had to be between 25 and 75 years old, have no history of severe autoimmune diseases, and have undergone dental implant treatment within a specified time frame. Only patients who agreed to participate in the study and provided informed consent were considered.

Patients with severe systemic conditions that could influence the osseointegration of implants, as well as those under chronic treatment with immunosuppressive drugs, were excluded. Also, patients who did not adhere to the post-operative monitoring schedule or could not provide complete data for analysis were not included in the study.

5.3.7. Conclusions

The results of this study provide a detailed perspective on the risk factors and post-operative complications associated with dental implants. The statistical analysis highlighted the negative impact of variables such as smoking, diabetes, hypertension, body mass index, compliance with post-operative instructions, and the number of implants on the outcomes of implant treatments.

This underlines the importance of a multidisciplinary approach in implant dentistry, including a detailed evaluation of risk factors, personalized prevention strategies, and proper post-operative monitoring.

Further studies are needed to explore the long-term effects of these risk factors and to identify new strategies to prevent complications. The integration of advanced technologies, such as the use of optimized biomaterials and regenerative therapies, could represent promising directions for improving the success of implant treatments.

CHAPTER 6. Zn_2SnO_4@SiO_2@5-FU NANOPARTICLES: A MULTIFUNCTIONAL ADDITIVE FOR MAXILLARY BONE RECONSTRUCTION WITH ANTIMICROBIAL AND ANTITUMORAL PROPERTIES

The primary objective of this study was the development and characterization of multifunctional Zn_2SnO_4@SiO_2@5-FU nanoparticles as an additive for bone-filling materials intended for maxillofacial dental reconstruction. The research aimed to evaluate the structural integrity, biocompatibility, antimicrobial efficacy, and antitumor potential of these modified

nanoparticles. By addressing the limitations of conventional materials used in bone regeneration, this study contributes to the advancement of biomaterial technologies, facilitating the development of more efficient and innovative solutions for reconstructive dental applications.

6.3. Results

6.3.2. Scanning Electron Microscopy

SEM micrographs show that Zn_2SnO_4 particles exhibit a predominantly spherical morphology, formed through the aggregation of nanorods, as illustrated in Figure 2 at magnifications of 25,000× and 50,000×. The particles show a pronounced tendency to agglomerate and display a high degree of dimensional uniformity, suggesting a high level of homogeneity in terms of shape. Dimensional analysis was performed for both spherical particles and nanorods, indicating average sizes of 1.17, 1.28, and 1.44 µm for the spherical particles, and 94.5, 114.68, and 106.48 nm for the nanorods.

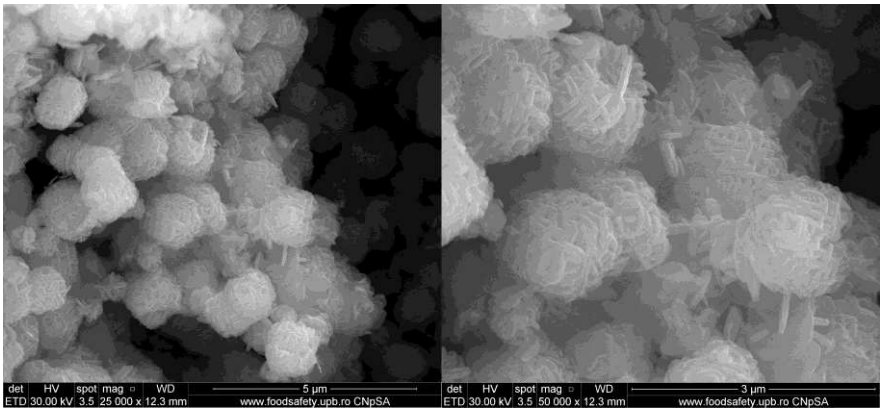

Figure 6.2. SEM Micrographs of Zn_2SnO_4.

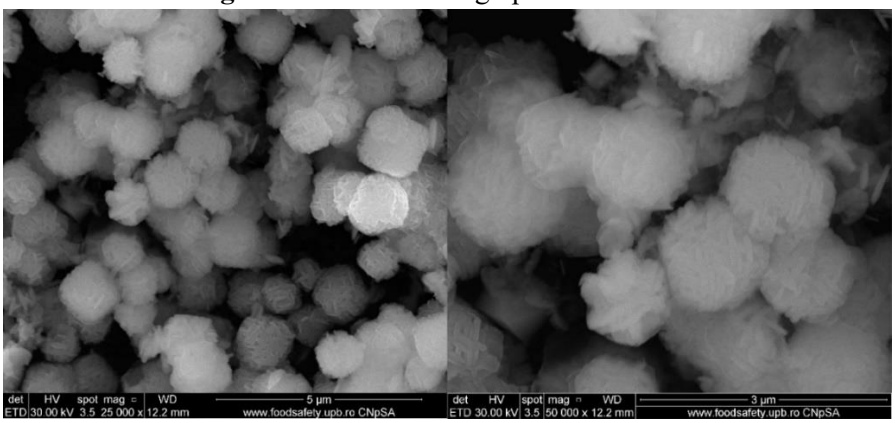

Figure 6.3. SEM Micrographs of Zn_2SnO_4@SiO_2.

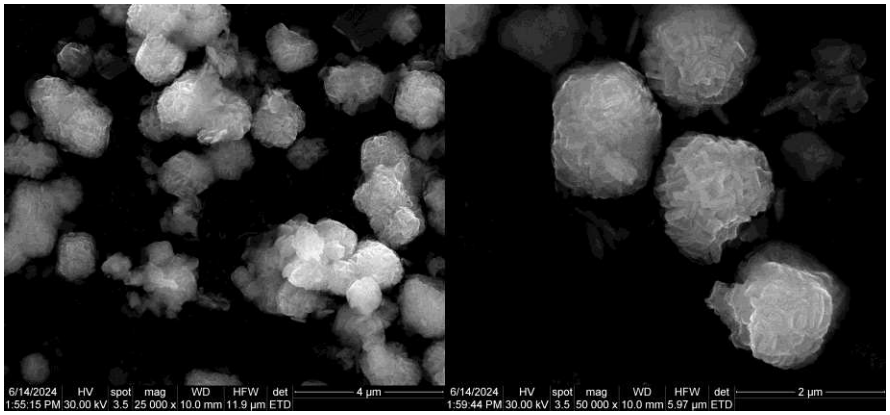

Figure 6.4. SEM Micrographs of Zn_2SnO_4@SiO_2@5-FU.

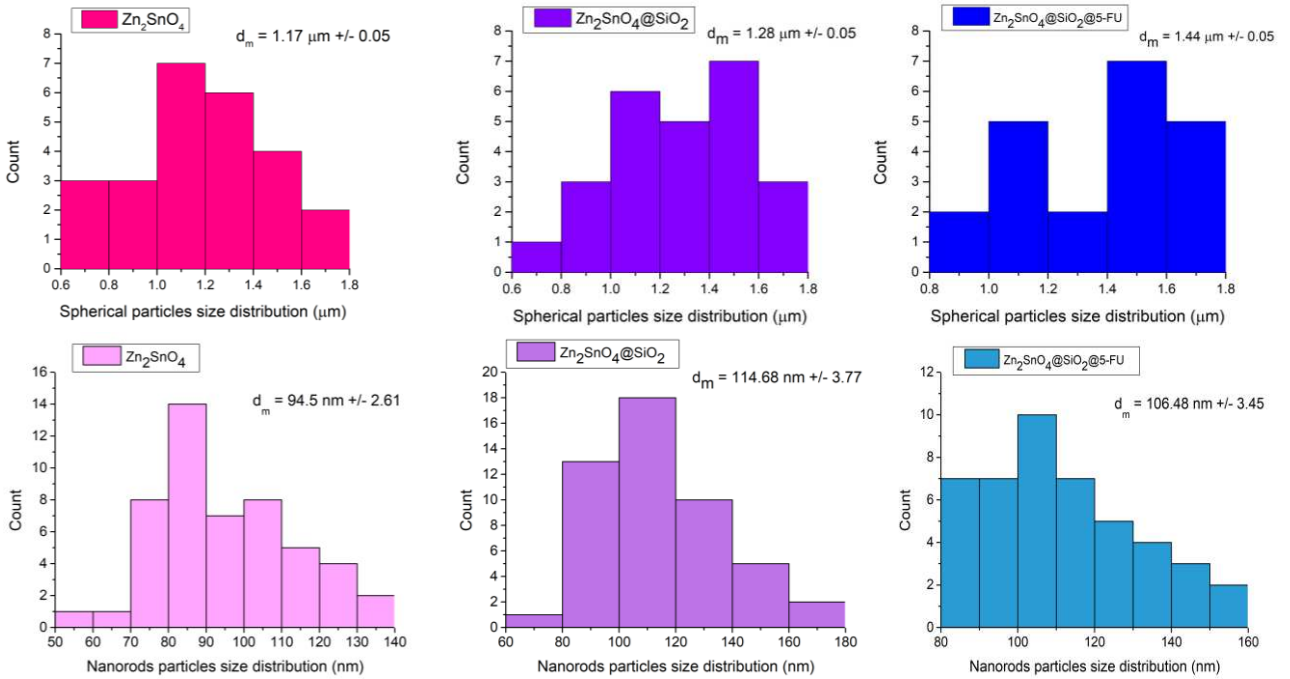

Figure 6.5. Particle size distribution for both spheres (µm) and nanorods (nm), calculated from the corresponding SEM images for each material. Size measurements were performed using ImageJ V 1.53 software, analyzing multiple images to ensure accuracy and reproducibility of the results.

After SiO_2 coating, a protective layer becomes visible on the particle surfaces, as observed in Figure 3. Following functionalization with 5-FU, the coating appears more defined, as shown in Figure 4, suggesting a direct interaction between 5-FU and the silica layer, resulting in a denser and more uniform coating around the particles.

An important observation is that the addition of the silica layer and incorporation of 5-FU does not significantly alter the size or morphology of the Zn_2SnO_4 particles, indicating that the coating and functionalization processes do not affect the structural integrity of the nanoparticles. Figure 6.5 illustrates the dimensional distribution for both spherical particles and nanorod aggregates, highlighting the morphological consistency of the synthesized materials.

6.3.3. Energy Dispersive X-ray Spectroscopy

SEM characterization was complemented by Energy Dispersive X-ray Spectroscopy, which enables compositional analysis and elemental mapping of the samples, revealing the distribution of each component element.

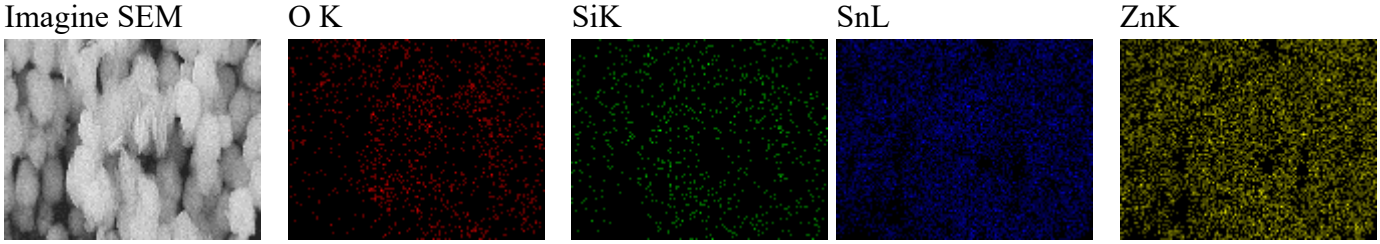

Figure 6.6. Elemental Mapping of Zn_2SnO_4@SiO_2.

Figure 6.6 shows elemental mapping for Zn_2SnO_4@SiO_2, confirming the presence of oxygen (O), silicon (Si), tin (Sn), and zinc (Zn). Each element is highlighted with distinct colors, validating the chemical composition of the material. The EDS spectra further support these identifications, displaying characteristic peaks for each detected element. The analysis results indicate a

homogeneous distribution of the elements across the sample, demonstrating a uniform SiO_2 coating on the Zn_2SnO_4 nanoparticles and confirming the success of the coating process.

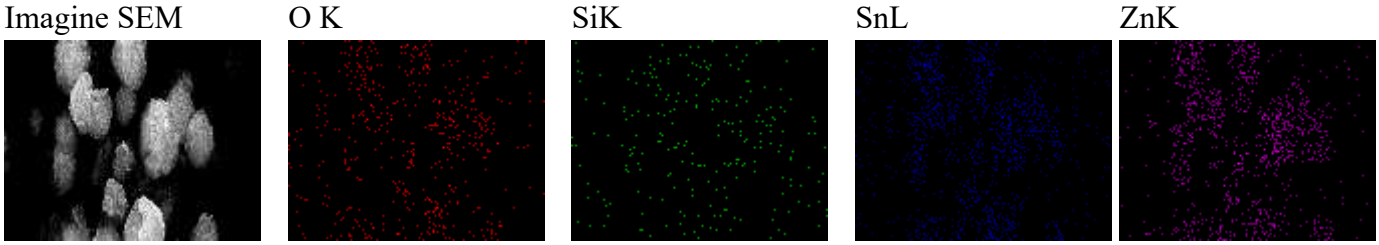

Figure 6.7. Elemental Mapping of Zn_2SnO_4@SiO_2@5-FU.

Similarly, Zn_2SnO_4@SiO_2@5-FU underwent EDS analysis, with comparable results in terms of elemental composition. Figure 6.7 shows the elemental mapping for this sample, again confirming the presence of oxygen, silicon, tin, and zinc, each represented by distinct colors. The EDS spectra suggest that the inclusion of 5-FU does not significantly alter the elemental composition of the sample, maintaining the characteristics previously observed in Zn_2SnO_4@SiO_2. This finding, corroborated by FTIR analysis, suggests that 5-FU is physically adsorbed onto the surface of Zn_2SnO_4@SiO_2, without forming new chemical bonds. This type of interaction could influence the controlled release of the drug in biomedical applications.

6.3.4. Fourier-Transform Infrared Spectroscopy

FTIR analysis provides essential information about the vibrational characteristics of chemical bonds within the material, allowing for the identification of functional groups and the confirmation of structural modifications. FTIR measurements for all samples were conducted over a spectral range between 400 cm^{-1} and 4000 cm^{-1}, offering relevant details about the chemical composition and molecular interactions. The obtained spectra, presented in Figure 6.8, highlight the presence and distribution of specific functional groups in each sample, providing a detailed characterization of Zn_2SnO_4, Zn_2SnO_4@SiO_2, and Zn_2SnO_4@SiO_2@5-FU.

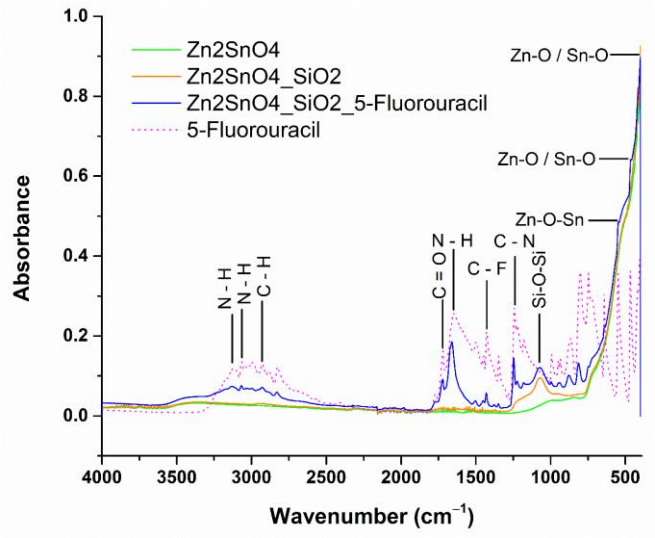

Figure 6.8. FTIR Spectra for Zn_2SnO_4, Zn_2SnO_4@SiO_2, Zn_2SnO_4@SiO_2@5-FU, and 5-FU.

The FTIR analysis of the zinc stannate (Zn_2SnO_4) sample reveals a prominent vibrational band at 590 cm^{-1}, attributed to the symmetric stretching vibration of ZnO and SnO_2, confirming the presence of the Zn–O–Sn bond characteristic of Zn_2SnO_4. This absorption band supports the successful formation of zinc stannate. Additionally, bands identified at 463 cm^{-1} and 400 cm^{-1} are

associated with Zn–O and Sn–O bonds, respectively, further validating the synthesis of Zn_2SnO_4. These vibrational bands are consistently observed across all synthesized samples, confirming that zinc stannate remains the primary component in the obtained formulations [17,18].

In the cases of Zn_2SnO_4@SiO_2 and Zn_2SnO_4@SiO_2@5-FU, the presence of a distinct band at 1072 cm^{-1} is attributed to the vibration of the Si–O–Si functional group, indicating the successful coating with SiO_2. The functionalization of Zn_2SnO_4@SiO_2@5-FU with 5-FU is confirmed by the appearance of several absorption bands corresponding to the reference spectrum of 5-FU.

The following characteristic vibrations of 5-FU were identified: N–H bending vibrations at 3130 cm^{-1} and 3067 cm^{-1}, along with a similar band at 1600 cm^{-1}, confirming the presence of the 5-FU structure; C–H stretching vibration at 2929 cm^{-1}; C=O functional group displaying a distinct band at 1772 cm^{-1}; C–F stretching vibration detected at 1430 cm^{-1}; A band at 1240 cm^{-1} attributed to the C–N bond [19,20]. These results successfully validate the functionalization process and confirm the presence of 5-FU in the final composite material.

6.3.6. Evaluation of Antimicrobial Profile

The Minimum Inhibitory Concentration (MIC) values presented in Figure 6.11 confirm the antibacterial efficacy of Zn_2SnO_4-based nanoparticles against S. aureus (Gram-positive) and E. coli (Gram-negative). Among all tested samples, Zn_2SnO_4@SiO_2@5-FU exhibited the lowest MIC values, indicating superior antimicrobial activity. This improvement is attributed to the functionalization with 5-FU, which adds additional antimicrobial effects due to its chemotherapeutic and antibacterial properties. These results suggest that integrating 5-FU not only enhances the therapeutic efficiency of the nanoparticles but also contributes to an expanded antimicrobial activity, offering promising potential for advanced biomedical applications.

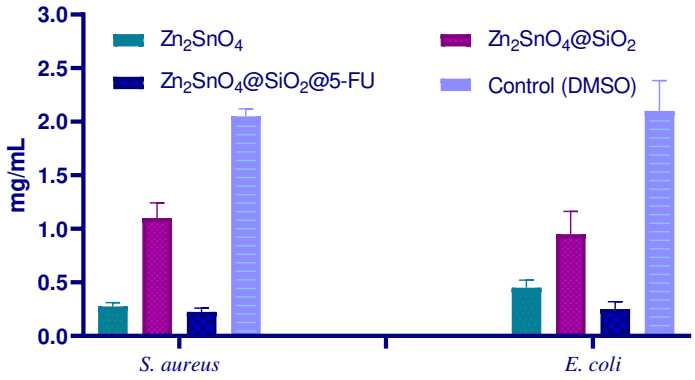

Figure 6.11. Minimum Inhibitory Concentration of Zn_2SnO_4, Zn_2SnO_4@SiO_2, and Zn_2SnO_4@SiO_2@5-FU against *S. aureus* and *E. coli*.

Despite its overall effectiveness, Zn_2SnO_4@SiO_2 showed slightly reduced antibacterial activity compared to Zn_2SnO_4, likely due to the silica layer partially protecting the nanoparticle core. This coating may limit the accessibility of Reactive Oxygen Species (ROS) and Zn^{2+}/Sn^{4+} ions, which are essential for the nanoparticles' antimicrobial mechanism.

A notable observation is that the MIC values obtained for E. coli were comparable to those for S. aureus, suggesting that the tested formulations are equally effective against both Gram-positive and Gram-negative bacteria, despite their structural differences.

The enhanced efficacy of Zn_2SnO_4@SiO_2@5-FU against both strains highlights the potential of this multifunctional nanoparticle system for broad-spectrum antibacterial applications. Moreover, the control test with DMSO demonstrated significantly higher MIC values, confirming that the

observed antibacterial effects were exclusively due to the nanoparticle formulations and not the solvent.

These results underline the potential of Zn_2SnO_4@SiO_2@5-FU as a promising antibacterial agent capable of effectively inhibiting both Gram-positive and Gram-negative bacteria, making it a viable candidate for advanced biomedical applications.

The antimicrobial mechanism of Zn_2SnO_4@SiO_2@5-FU nanoparticles against Gram-positive and Gram-negative bacteria can be attributed to their distinct structural and functional characteristics.

In Gram-positive bacteria like S. aureus, the thick and porous peptidoglycan layer allows easier penetration of the nanoparticles and the reactive species they release. The Reactive Oxygen Species (ROS) generated by Zn_2SnO_4 interact with essential cellular structures, including the bacterial cell wall, proteins, and DNA, inducing oxidative stress that disrupts metabolic functions and compromises cell integrity [21,22].

In addition to ROS generation, the nanoparticles release Zn^{2+} and Sn^{4+} ions, which bind to sulfhydryl groups in membrane proteins, interfering with bacterial enzyme activities. This interaction destabilizes membrane structures and disrupts metabolic pathways, reducing bacterial viability [23,24].

Furthermore, 5-FU amplifies these effects by disrupting bacterial DNA synthesis, leading to the inhibition of cellular replication and eventual bacterial destruction. The synergy between oxidative stress, ion release, and the action of 5-FU explains the high antimicrobial efficiency of Zn_2SnO_4@SiO_2@5-FU nanoparticles against Gram-positive strains [25].

For Gram-negative bacteria like E. coli, the outer membrane composed of lipopolysaccharides (LPS) acts as a protective barrier, giving these bacteria higher intrinsic resistance to antimicrobial agents [26]. However, Zn_2SnO_4@SiO_2@5-FU nanoparticles can overcome this barrier through multiple mechanisms.

The ROS generated by the nanoparticles penetrate the outer membrane, causing oxidative damage to lipids and structural proteins [20,24]. Simultaneously, Zn^{2+} and Sn^{4+} ions interact with the negatively charged LPS molecules, destabilizing the outer membrane and increasing its permeability [23,26].

This destabilization facilitates the entry of nanoparticles and 5-FU into the periplasmic space, where they can traverse the thin peptidoglycan layer and directly interact with essential cellular structures. Specifically, 5-FU interferes with bacterial DNA synthesis and inhibits metabolic pathways crucial for cell division, amplifying the antimicrobial effect [25,27]. Through these synergistic mechanisms, Zn_2SnO_4@SiO_2@5-FU nanoparticles demonstrate comparable efficacy against both Gram-positive and Gram-negative bacteria, positioning them as a broad-spectrum antimicrobial agent with significant potential for advanced biomedical applications [27].

6.3.7. Evaluation of Cytotoxic Activity

To assess the cytotoxic activity of Zn_2SnO_4, Zn_2SnO_4@SiO_2, and Zn_2SnO_4@SiO_2@5-FU powders on the human epidermoid carcinoma cell line A-431, the cells were treated for 24 hours with varying concentrations of these nanoparticles. After treatment, cellular metabolic activity was evaluated using the MTT spectrophotometric assay to determine the cytotoxicity of each sample on the A-431 tumor cells.

The cytotoxicity results (Figure 6.12) showed that all Zn_2SnO_4-based samples exerted a toxic effect on A-431 cells, with cytotoxicity increasing in a dose-dependent manner. Although all three powders significantly reduced cell viability at both high and moderate concentrations, a marked

decrease in cell viability was observed at 37.5 µg/mL. At a concentration of 1.5 µg/mL, no significant cytotoxic effect was detected compared to the untreated control for any of the samples.

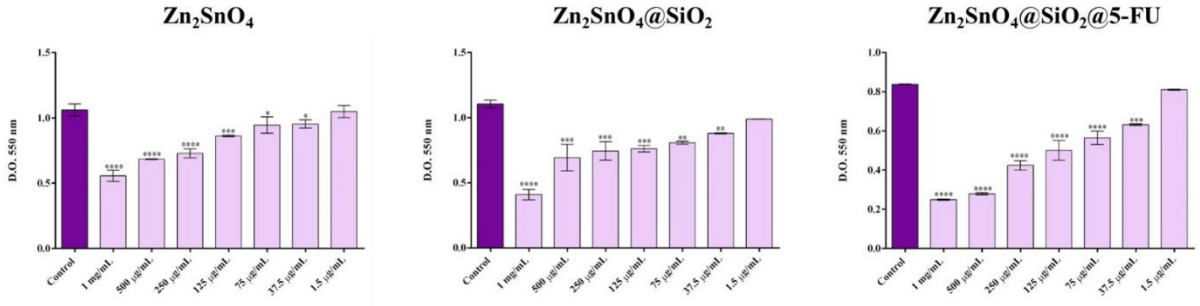

Figure 6.12. Viability of A-431 tumor cells after 24 hours of treatment with varying concentrations of Zn_2SnO_4, Zn_2SnO_4@SiO_2, and Zn_2SnO_4@SiO_2@5-FU powders ($p \leq 0.0001$ for control vs. sample, $^{**}p \leq 0.001$, $^{*}p \leq 0.01$, $p \leq 0.05$).

Despite some similarities in their cytotoxic profiles, Zn_2SnO_4@SiO_2@5-FU demonstrated the strongest cytotoxicity, leading to a more significant reduction in cell viability than Zn_2SnO_4 and Zn_2SnO_4@SiO_2 at equivalent concentrations. At the highest tested concentration (1 mg/mL), Zn_2SnO_4 reduced cell viability by approximately 1.9 times compared to the control, Zn_2SnO_4@SiO_2 by 2.75 times, and Zn_2SnO_4@SiO_2@5-FU by 3.45 times, demonstrating significant cytotoxicity even at lower concentrations.

These results highlight the synergistic effect of 5-FU functionalization, which amplifies the antitumor impact of Zn_2SnO_4 nanoparticles through combined mechanisms, including ROS-induced oxidative stress, ionic release, and the direct inhibition of DNA synthesis by 5-FU.

The cytotoxicity data were used to estimate the Lethal Dose 50 (LD_{50}), the concentration required to destroy 50% of the exposed cells. The results indicate that the LD_{50} for Zn_2SnO_4 was approximately 1 mg/mL, while for Zn_2SnO_4@SiO_2, the exact value could not be precisely determined but ranged between 500 µg/mL and 1 mg/mL. In contrast, for Zn_2SnO_4@SiO_2@5-FU, the LD_{50} was significantly lower, at 250 µg/mL, highlighting a superior cytotoxic potential due to the presence of 5-FU.

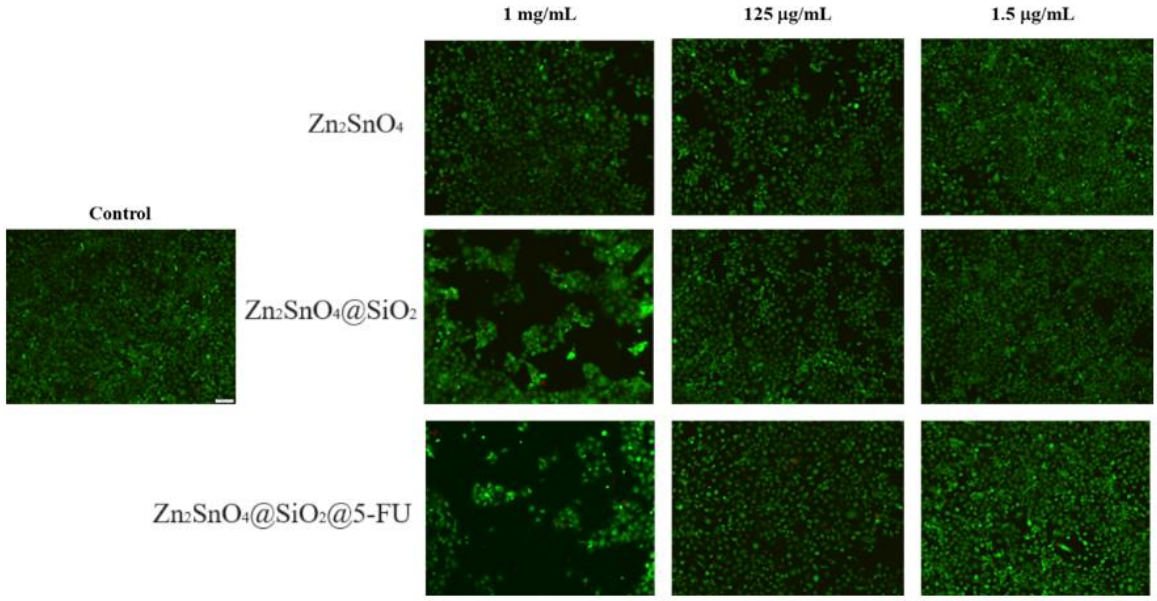

Figure 6.13. Fluorescence microscopy images showing live (green) and dead (red) A-431 tumor cells after 24 hours of treatment with different concentrations of Zn_2SnO_4, Zn_2SnO_4@SiO_2, and Zn_2SnO_4@SiO_2@5-FU powders (10× magnification).

Fluorescence microscopy using Live/Dead staining for A-431 tumor cells confirmed these results, as seen in Figure 6.13. Zn_2SnO_4 powder exhibited moderate cytotoxic effects compared to the untreated control. In the case of Zn_2SnO_4@SiO_2 treatment, a visible decrease in cell viability was observed, with cells losing the compact cluster formation characteristic of tumor organization. The strongest cytotoxic effect was observed for Zn_2SnO_4@SiO_2@5-FU, particularly at higher concentrations (1 mg/mL), where a significant reduction in the number of viable cells was noted. Treated cells were organized into small, dispersed clusters, in clear contrast to the control sample.

These results confirm that functionalization with 5-FU significantly enhances the antitumor activity of the nanoparticles, reinforcing their potential for advanced biomedical applications in oncological therapies.

CHAPTER 7. NANOSTRUCTURED COATINGS BASED ON PMMA/ZnO(NanoAg) APPLIED ON DENTAL IMPLANT ABUTMENTS: SYNTHESIS, CHARACTERIZATION, AND EVALUATION

In this study, we investigated the development of an innovative material designed for coating the surfaces of dental implant abutments, based on a **polymethyl methacrylate (PMMA)** polymer matrix enriched with **zinc oxide (ZnO)** and **silver (Ag)** nanoparticles. Recent studies have demonstrated the considerable efficacy of these nanoparticles in preventing bacterial biofilm formation through mechanisms that directly target microbial cells and disrupt their essential processes [28-31]. The integration of these nanoparticles into the PMMA matrix results in a stable and durable surface treatment capable of maintaining sustained long-term antimicrobial activity.

7.3. Results

7.3.1. Characterization of Powder Samples—ZnO and ZnO-Ag

7.3.1.3. Scanning Electron Microscopy

Figures 7.3 and 7.4 provide detailed information regarding the morphology and size of the synthesized nanoparticles.

The SEM micrographs for the zinc oxide sample, taken at three distinct magnifications (50,000×, 100,000×, and 200,000×), confirm the formation of quasi-spherical nanoparticles characterized by uniform morphology and a homogeneous size distribution. The hydrothermal synthesis parameters were precisely controlled to prevent excessive nanoparticle growth, resulting in particles with an average size of 30.36 ± 0.8 nm.

Although the nanoparticles exhibit a natural tendency to agglomerate, they retain well-defined edges and distinct morphologies, indicating a stable structure. Additionally, energy-dispersive X-ray spectroscopy (EDS) analysis confirms the presence of zinc and oxygen in the sample, supporting previous findings regarding the composition and purity of the synthesized material.

The SEM results for the ZnO-Ag composite nanoparticles are shown in Figure 7.4.

The images highlight subtle differences compared to the pure zinc oxide sample, particularly the presence of smaller particles distributed homogeneously throughout the sample, attributed to silver nanoparticles. The micrographs were captured at the same three magnifications used for the control sample, allowing for direct comparison of the observed morphologies.

In the micrograph taken at 50,000× magnification, the use of backscattered electron detection revealed areas with varying brightness. The brighter regions correspond to silver due to its higher atomic number and density compared to zinc.

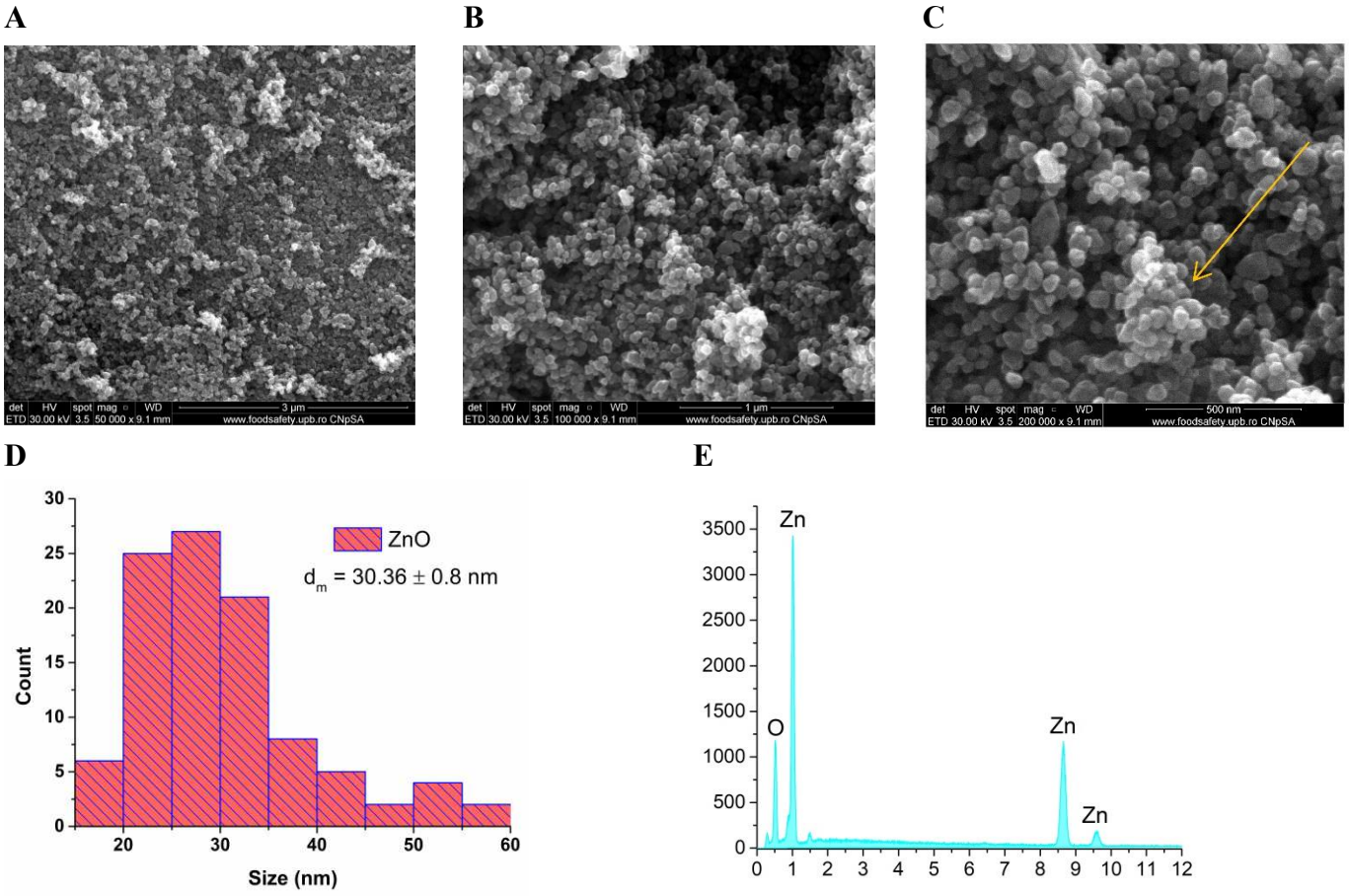

Figure 7.3. SEM micrographs of zinc oxide nanoparticles recorded at magnifications of (A) 50,000×, (B) 100,000×, and (C) 200,000×, (D) particle size distribution, and (E) EDS results for ZnO nanoparticles.

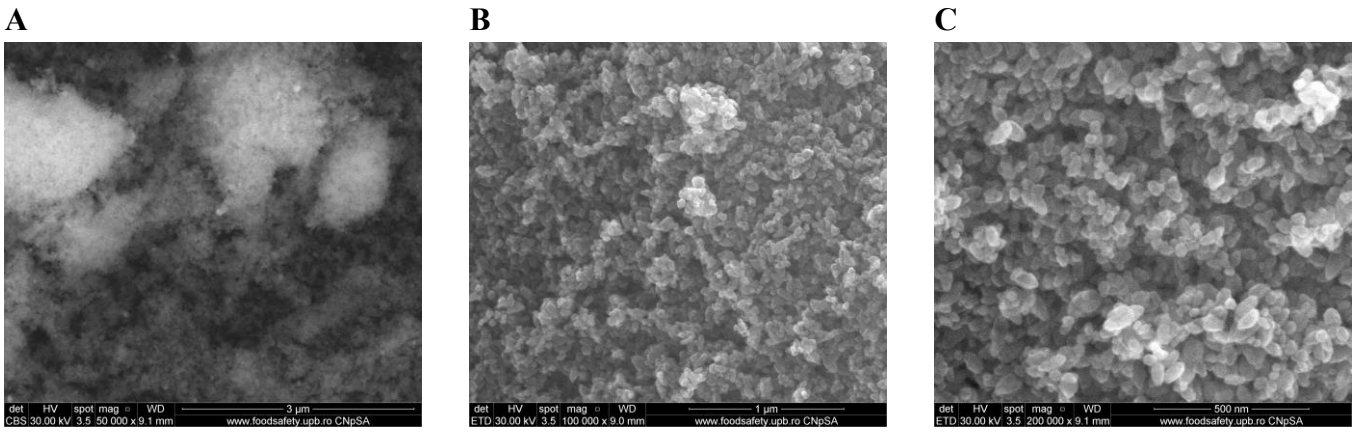

E

D

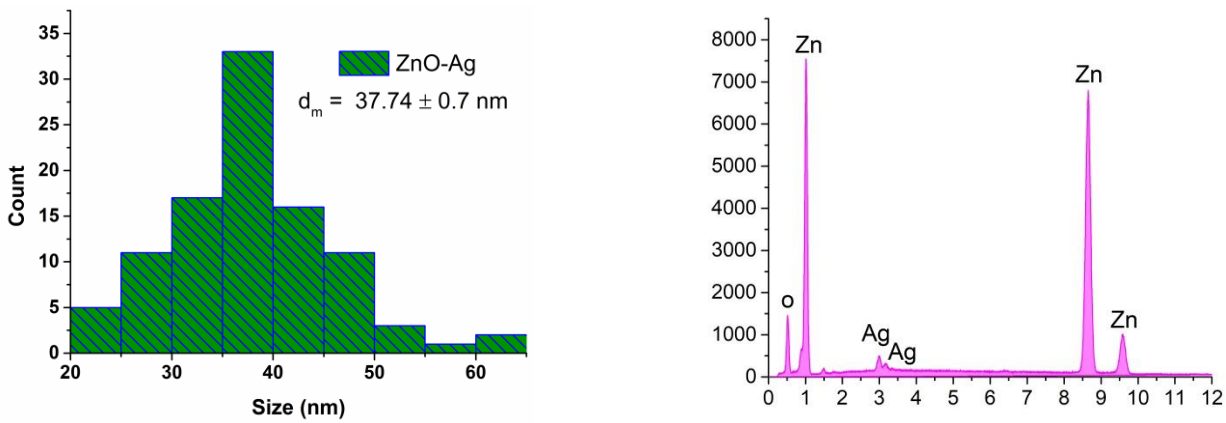

Figure 7.4. SEM micrographs at magnifications of (A) 50,000×, (B) 100,000×, and (C) 200,000×, (D) particle size distribution, and (E) EDS results for ZnO-Ag nanoparticles.

Although the addition of silver does not significantly alter the overall morphology of the particles, it causes a slight increase in the average particle size, measured at 37.74 ± 0.7 nm. Moreover, the presence of silver in the composite sample is confirmed through elemental analysis, with the EDS spectrum clearly indicating the presence of silver within the material's structure.

7.3.2. Characterization of Coating Samples—PMMA, PMMA ZnO, PMMA ZnO-Ag

7.3.2.1. Infrared Microscopy

Following the deposition of nanostructured coatings based on PMMA enriched with zinc oxide (ZnO) and zinc-silver oxide (ZnO-Ag) nanoparticles, the samples underwent a series of physicochemical analyses to achieve a detailed characterization of the obtained materials.

Given the proposed application, the first stage of investigation involved infrared (IR) microscopy analysis, which provided essential information about the uniformity of the coatings and facilitated the identification of specific functional groups within each deposited layer. This technique enabled the evaluation of the homogeneous distribution of the components within the polymer matrix and confirmed the interactions between PMMA and the incorporated nanoparticles. Figures 7.5–7.7 present the FTIR microscopy results for the nanostructured PMMA, PMMA-ZnO, and PMMA-ZnO-Ag coatings applied on titanium alloy substrates.

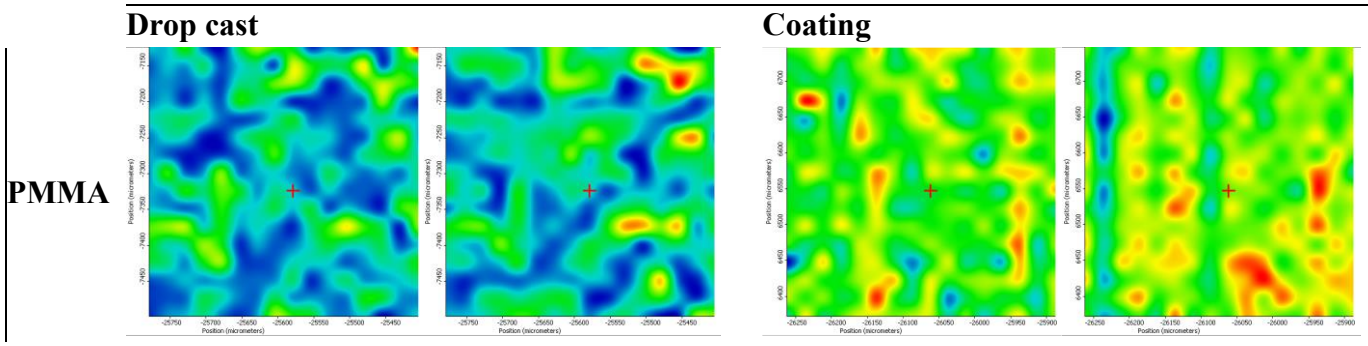

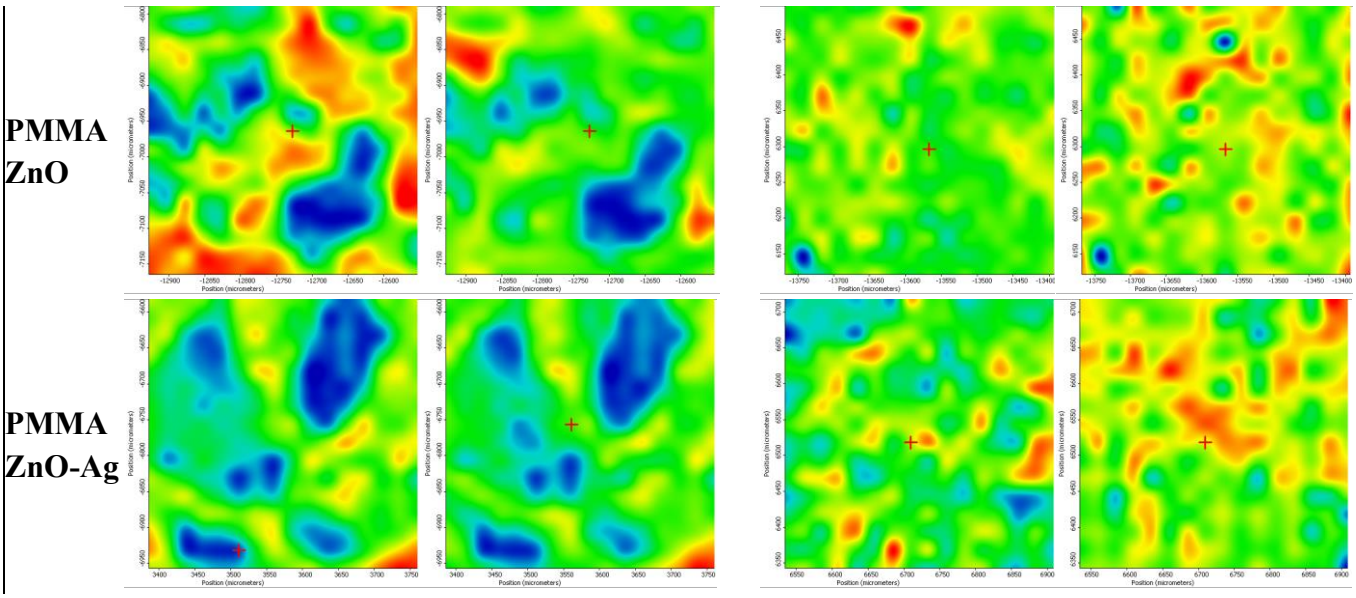

Figure 7.5. IR mapping for drop-cast and nanostructured coatings based on PMMA, PMMA ZnO, and PMMA ZnO-Ag.

The maps generated from the analysis of the three samples—both those deposited via drop-casting and the thin films based on PMMA with antimicrobial nanoparticles—highlight chromatic variations, reflecting the degree of coverage and uniformity of the coating.

For the drop-cast samples, the presence of extensive blue-colored regions indicates a low level of coverage. In contrast, the nanostructured coatings obtained through spin-coating exhibit distinct chromatic distributions across the different samples. The PMMA control layer shows color transitions from green to yellow, with isolated areas in orange-red shades.

The sample containing zinc oxide nanoparticles presents noticeable differences compared to the control layer, including an increased prevalence of red regions, suggesting changes in material composition and distribution. Conversely, the PMMA-ZnO-Ag sample demonstrates superior homogeneity in stratification, indicating enhanced integration and a more uniform coating of the titanium alloy substrate.

The IR maps correlate with the IR spectra obtained, which highlight the presence of functional groups characteristic of the PMMA polymer matrix. Specifically, absorption bands at 2994 cm^{-1} and 2950 cm^{-1} are attributed to the stretching vibrations of C-H bonds associated with methyl and methylene groups. Additionally, the absorption band observed at 1729 cm^{-1} corresponds to the carboxylate group in the acrylic structure, while the signal at 1149 cm^{-1} is associated with the stretching vibration of the C-O-C bond.

7.3.2.2. Scanning Electron Microscopy and Energy Dispersive X-ray Spectroscopy

The thin PMMA-based coatings applied to the titanium alloy substrate were characterized using scanning electron microscopy (SEM) to evaluate the distribution and uniformity of the surface layers. Additionally, energy-dispersive X-ray spectroscopy (EDS) was employed to analyze the elemental composition, providing detailed information on the presence and distribution of components within the deposited layer (Figure 7.7).

The SEM image of the titanium alloy substrate revealed a pronounced surface roughness characteristic of the support material. EDS analysis confirmed the elemental composition of the alloy, verifying the presence of its primary constituents. In the PMMA-coated sample, a distinct alteration

in surface characteristics was observed compared to the uncoated substrate, with the polymer layer showing uniform distribution and continuous deposition.

For the ZnO nanoparticle-containing sample, SEM analysis revealed a homogeneous integration of nanoparticles within the polymer matrix, though some agglomeration was observed in specific regions of the coating.

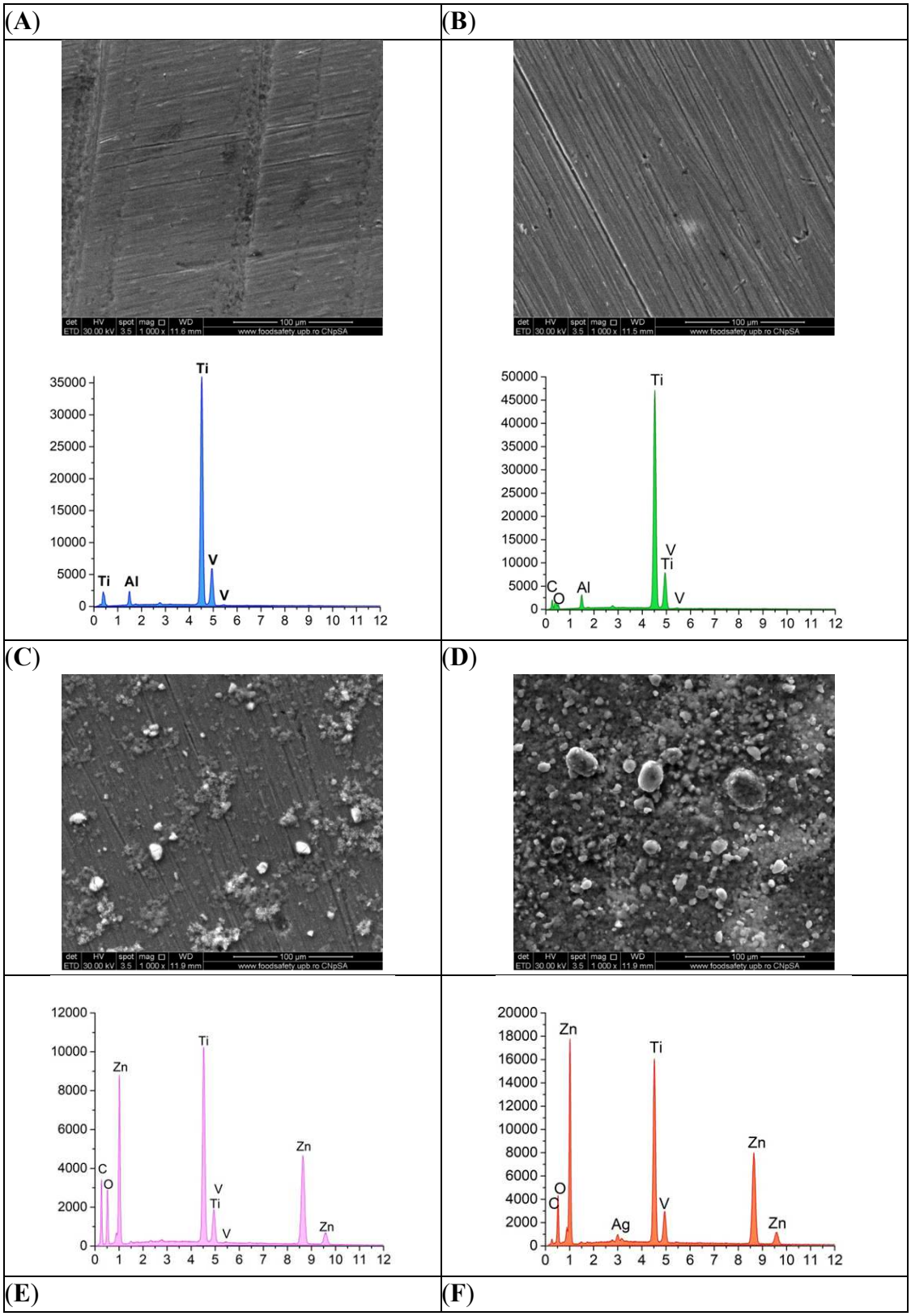

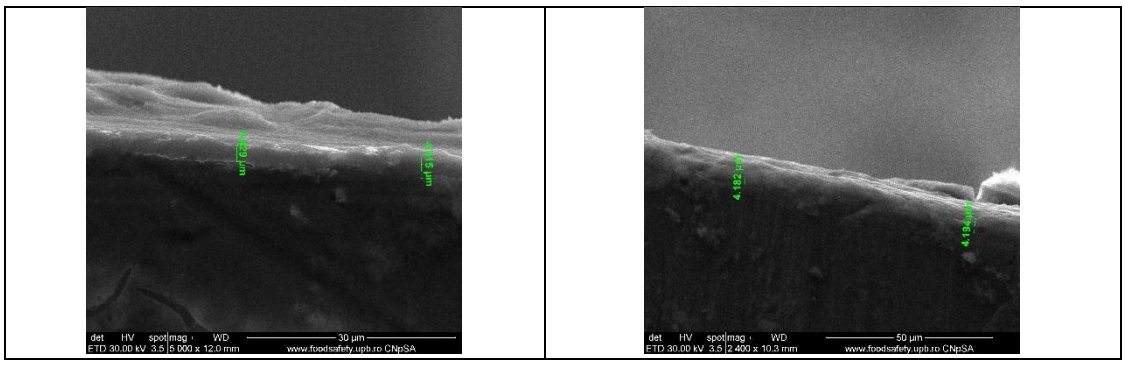

Figure 7.7. EM micrographs and EDS spectra for: (A) Uncoated Ti6Al4V substrate, (B) PMMA-coated substrate, (C) PMMA ZnO coating, (D) PMMA ZnO-Ag coating, (E) Cross-section of PMMA ZnO, (F) Cross-section of PMMA ZnO-Ag

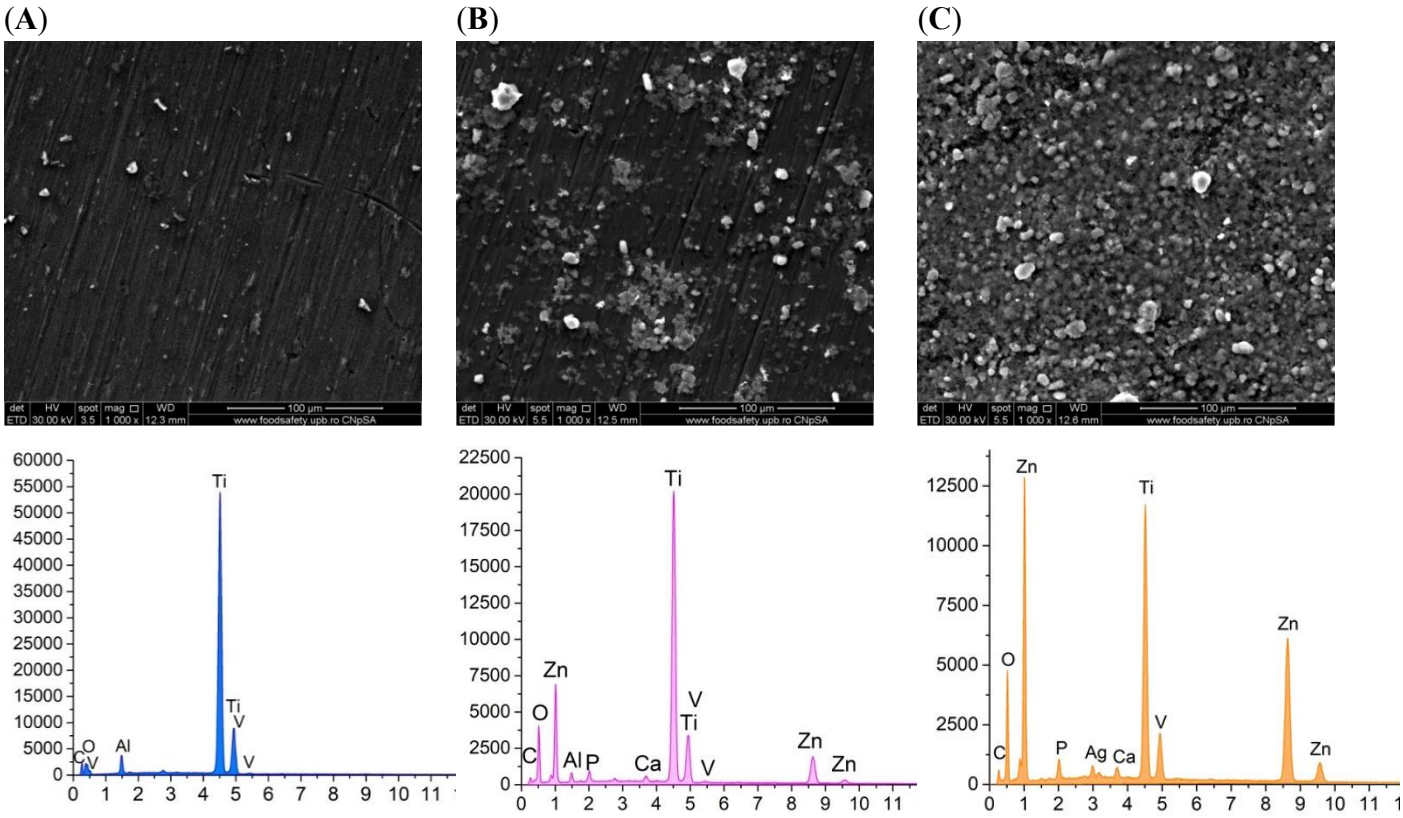

Figure 7.8. SEM micrographs and EDS spectra for: (A) PMMA layer, (B) PMMA ZnO layer, (C) PMMA ZnO-Ag layer after 7 days of immersion in SBF.

The ZnO-Ag composite layer exhibited significant differences compared to the other samples, including an increased density of nanoparticles within the deposited layer. This sample displayed a more uniform nanoparticle distribution throughout the polymer matrix, contributing to enhanced continuity and integrity of the nanostructured coating.

Cross-sectional SEM images (Figure 7.7 E, F) revealed variations in the thickness of the coatings, with PMMA-ZnO layers measuring between 2 and 4 μm and PMMA-ZnO-Ag layers ranging from 4 to 5 μm. EDS analysis confirmed the presence of carbon and oxygen (from PMMA), as well as zinc and silver in the respective samples, along with elements from the titanium alloy substrate. These findings support the uniformity and consistency of the coatings in the studied samples.

To assess the interaction of the materials with a simulated physiological environment, the samples were analyzed using SEM and EDS after immersion in simulated body fluid (SBF), prepared according to Kokubo's recipe. The samples were immersed in SBF at 37°C in a thermostatic bath, with evaluations conducted after 7, 14, and 21 days. After each period, the samples were extracted, washed, and analyzed to investigate the coating's interaction with the simulated environment.

The primary objective of this analysis was to monitor the crystallization of calcium phosphates on the surface, an essential indicator of the bioactivity of the tested materials. Figures 7.8–7.10 present the SEM and EDS results for the three immersion intervals.

In the control samples coated only with PMMA, SEM images after 7, 14, and 21 days at 37°C showed the presence of heterogeneous deposits on the surface. EDS compositional analysis indicated that after 7 and 14 days, the elemental composition of the surface remained similar to its initial state before immersion, with minimal signs of calcium phosphate crystallization, suggesting low bioactivity for the pure PMMA coatings. In contrast, coatings containing ZnO and ZnO-Ag nanoparticles exhibited clear signs of calcium phosphate crystallization after immersion, particularly in the PMMA ZnO-Ag sample, where more extensive and uniform mineralization was observed. This suggests enhanced bioactivity, likely due to the synergistic effects of zinc and silver nanoparticles in promoting hydroxyapatite formation, an essential component for bone integration in dental applications.

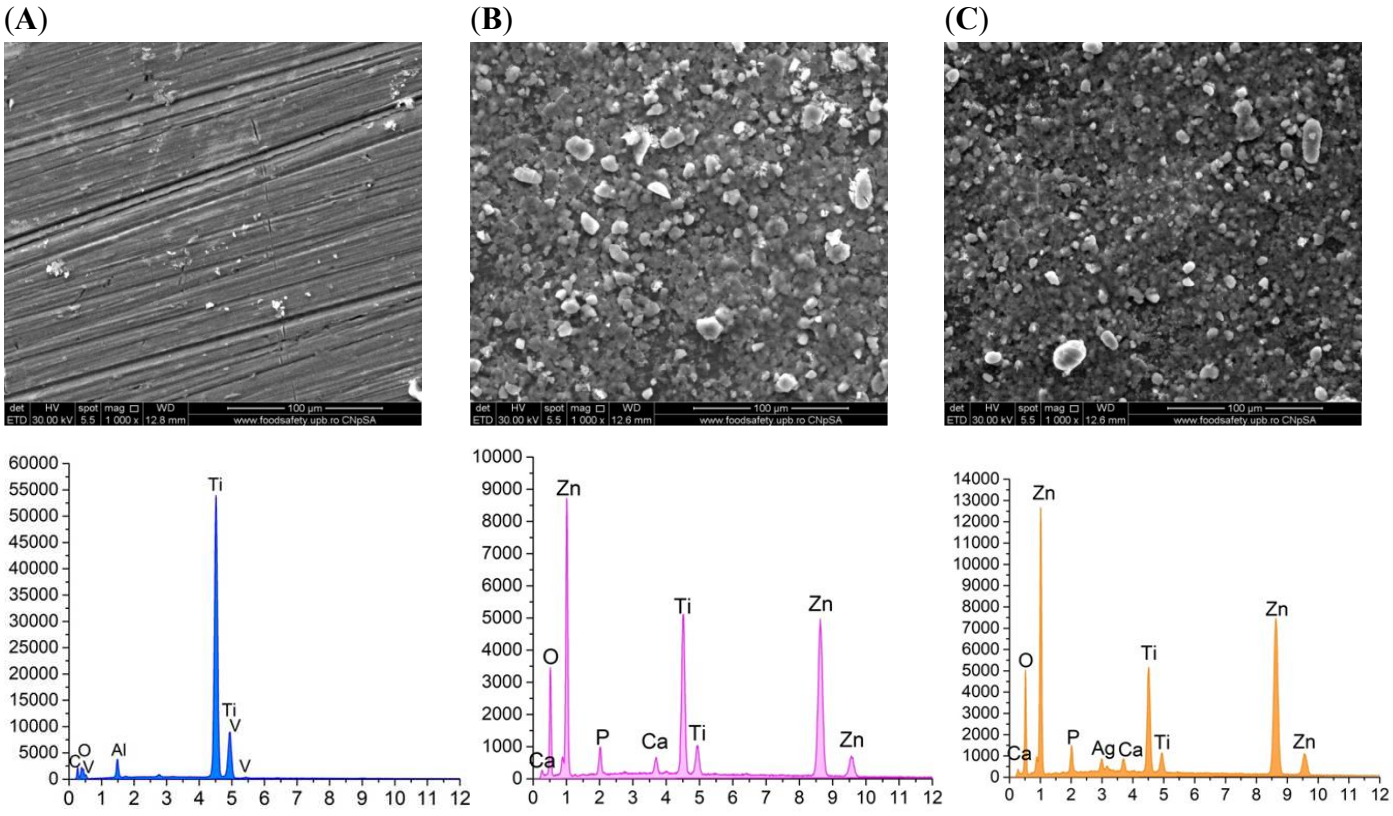

Figure 7.9. SEM Micrographs and EDS Spectra for PMMA Layer (A), PMMA ZnO Layer (B), and PMMA ZnO-Ag Layer (C) after 14 Days of Immersion in SBF.

After 21 days of immersion, the EDS spectra revealed the presence of new elements, particularly calcium and phosphorus, suggesting that the PMMA layer required a longer period to facilitate the calcium phosphate crystallization process. This phenomenon highlights the bioactive potential of the material, albeit at a slower rate compared to other tested formulations.

In contrast, substrates coated with PMMA enriched with zinc oxide nanoparticles exhibited progressive formation of granulations on the surface throughout the immersion period. This indicates that the zinc oxide nanoparticles impart superior bioactivity to the material, promoting the nucleation and growth of calcium phosphates when in contact with the simulated body fluid (SBF).

To support this observation, the energy-dispersive X-ray spectroscopy (EDS) analysis confirmed the presence of calcium and phosphorus, alongside the characteristic elements of the analyzed coating. A comparison of results showed that while the initial signs of calcium phosphate formation were detected after 7 days of immersion, the intensity of signals associated with these elements significantly increased after 14 and 21 days. This increase correlates with microscopic changes observed on the surface of the samples, indicating a progressive accumulation of mineral deposits and confirming the enhanced bioactive potential of the material.

The PMMA ZnO-Ag coating demonstrated even greater mineral deposition, suggesting that the synergistic effects of zinc and silver nanoparticles further improved the bioactivity of the composite, leading to faster and more uniform calcium phosphate crystallization. These findings emphasize the importance of nanoparticle incorporation in enhancing the biofunctional properties of PMMA-based coatings for biomedical applications, particularly in dental implantology.

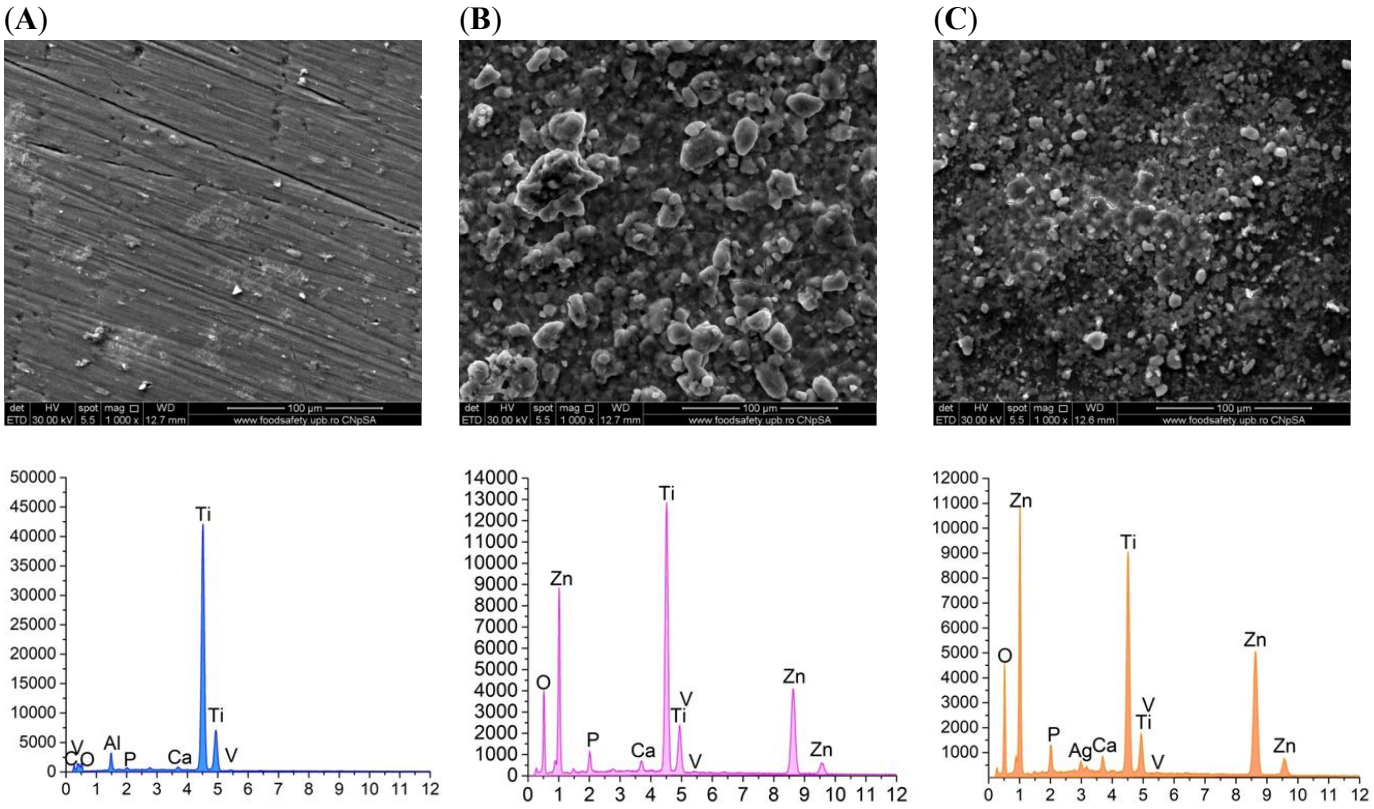

Figure 7.10. SEM Micrographs and EDS Spectra for PMMA Layer (A), PMMA ZnO Layer (B), and PMMA ZnO-Ag Layer (C) after 21 Days of Immersion in SBF

The samples coated with PMMA-based layers incorporating zinc-silver oxide composite nanoparticles demonstrated a progressive formation of calcium phosphates, with the process remaining strongly dependent on the duration of exposure in the simulated body fluid (SBF). A noteworthy observation is that the presence of zinc-silver oxide composite nanoparticles appears to reduce the granular agglomeration tendency observed in the ZnO-only coatings, leading to the formation of a more uniform crystalline film on the substrate surface.

The bioactivity of these samples was further confirmed through energy-dispersive X-ray spectroscopy (EDS) analysis, which consistently indicated the presence of calcium and phosphorus across all three time intervals studied. These findings support the material's potential to promote mineralization processes, reinforcing its relevance for biomedical applications, particularly in contexts where enhanced bioactivity and integration with biological tissues are critical, such as in dental implants and bone regeneration.

The PMMA ZnO-Ag coatings not only facilitated uniform calcium phosphate deposition but also maintained a stable and continuous crystalline layer, highlighting the advantage of incorporating silver alongside zinc in the nanoparticle composition. This improvement in surface mineralization may contribute to better implant integration and enhanced long-term performance in biomedical applications.

7.3.2.3. Microbial Biofilm Development

The materials developed in this study were designed to be used as a protective layer for prosthetic abutments in a complete dental implant system. These nanostructured coatings were engineered to address the issue of post-implant infections while simultaneously providing a favorable environment for the process of osseointegration.

To evaluate the antimicrobial efficacy of the coatings, the samples underwent specific tests focusing on the dynamics of biofilm formation, particularly investigating the initial microbial adhesion to the substrate surface. The experiments were conducted over a 24-hour incubation period using a Gram-positive strain (*Staphylococcus aureus*), a Gram-negative strain (*Pseudomonas aeruginosa*), and a fungal strain (*Candida albicans*).

The results obtained are graphically represented in Figure 7.11, expressed in log10 CFU/mL. Interpretation of the results was performed by comparing the functionalized samples with the bacterial control and the PMMA sample, allowing for an evaluation of the influence of antimicrobial nanoparticles on inhibiting biofilm formation.

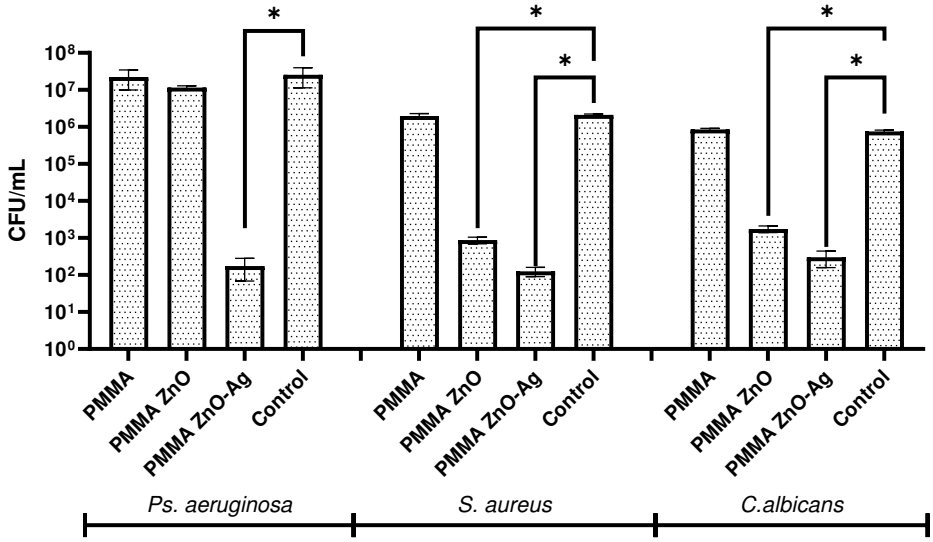

Figure 7.11. Graphical representation of biofilm modulation (log10 CFU/mL) for Gram-positive, Gram-negative, and fungal strains after 24 hours of incubation with PMMA, PMMA ZnO, and PMMA ZnO-Ag coatings; ($p \leq 0.05$, one-way ANOVA, samples vs. control).

The results highlight distinct biofilm formation patterns on the surface of the various tested samples. For the PMMA control sample, the number of adherent microorganisms was comparable to the untreated control, indicating the absence of significant antimicrobial effects. Among the tested

strains, *Pseudomonas aeruginosa* exhibited the highest biofilm formation, with CFU/mL values exceeding 10^7, confirming its strong adhesion and biofilm development capabilities. In contrast, *Staphylococcus aureus* and *Candida albicans* showed lower levels of biofilm formation, with CFU/mL values around 10^6 in the control samples.

The samples functionalized with zinc oxide nanoparticles (PMMA ZnO) demonstrated significant antimicrobial activity, particularly against *Staphylococcus aureus* and *Candida albicans*, reducing CFU/mL levels below 10^5 and 10^4, respectively, compared to the PMMA control. However, the inhibitory effect against *Pseudomonas aeruginosa* was limited, with CFU/mL values remaining around 10^6, suggesting a higher resistance to the action of zinc oxide. This reduced efficacy can be attributed to the intrinsic resistance mechanisms of *Pseudomonas aeruginosa*, including its outer membrane rich in lipopolysaccharides (LPS), which acts as a barrier, limiting the penetration of zinc oxide nanoparticles. Additionally, the complex matrix of extracellular polymeric substances (EPS) characteristic of biofilms formed by this species offers further protection against antimicrobial agents, emphasizing the need to optimize formulations for effectively combating Gram-negative bacteria.

The most notable results were obtained with the PMMA ZnO-Ag coated samples, which showed significant inhibition of biofilm formation for all tested strains, including *Pseudomonas aeruginosa*, *Staphylococcus aureus*, and *Candida albicans*. CFU/mL values for these samples were consistently reduced to approximately 10^3, indicating an almost complete inhibition of microbial proliferation. These findings confirm the synergistic effect of zinc oxide and silver nanoparticles, contributing to the effective prevention of biofilm formation within the first 24 hours of exposure.

The data obtained support the potential of PMMA ZnO-Ag coatings as effective antimicrobial surfaces with relevant biomedical applications, particularly in preventing infections associated with dental implants.

7.3.2.4. In Vitro Evaluation of the Impact of Nanostructured Coatings on Human Fibroblasts

To investigate the effect of nanostructured coatings on hFOB 1.19 cells, a series of in vitro analyses were conducted, focusing on cell viability, proliferation, cytotoxicity, and potential pro-inflammatory effects.

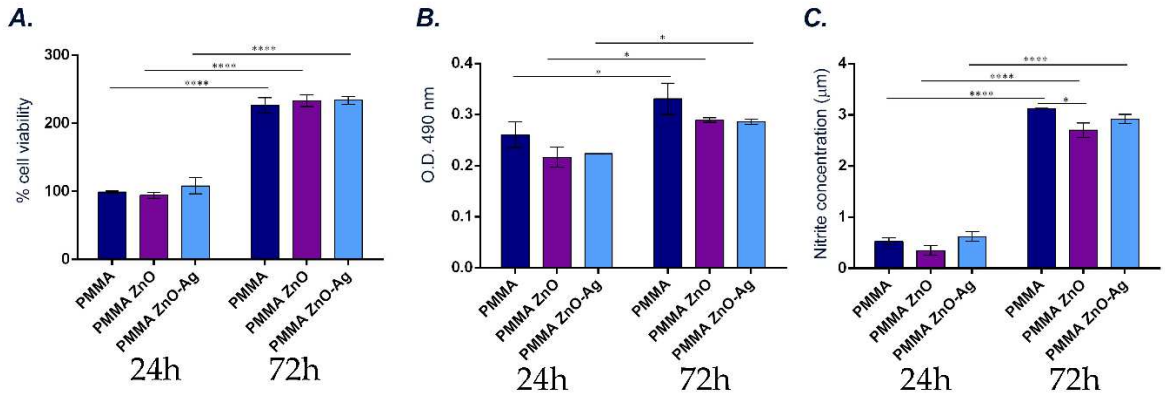

Figure 7.12. graphically presents the results for: (A) Cell viability and proliferation potential of human preosteoblasts after 24 and 72 hours of interaction with PMMA, PMMA/ZnO, and PMMA/ZnO(NanoAg) coatings. (B) Cytotoxic potential, measured by LDH quantification, under the same experimental conditions. (C) NO release, as a marker for oxidative stress and inflammatory responses, after 24 and 72 hours of interaction. Statistical significance is indicated as follows: $p \leq 0.05$, ***$p \leq 0.0001$. All experiments were performed in triplicate, and the results represent the mean of three independent experiments..

The results from the MTT assay (Figure 7.12A) indicated that after 24 hours of interaction between the cells and the materials, there were no significant differences in cell viability across the tested coatings. This suggests that the initial interaction of human preosteoblasts with the PMMA, PMMA/ZnO, and PMMA/ZnO-Ag surfaces did not negatively impact their metabolic activity. Extending the interaction period to 72 hours maintained the same viability profile, indicating that the integration of ZnO or ZnO-Ag into the PMMA matrix did not adversely affect cellular metabolism. Moreover, a statistically significant increase in cell viability was observed at 72 hours compared to 24 hours for all tested materials, suggesting that these coatings support the proliferation of human preosteoblasts over time.

To evaluate potential cytotoxic effects of the tested materials, lactate dehydrogenase (LDH) activity was quantified as an indicator of cell membrane integrity (Figure 7.12B). The results showed that LDH levels remained constant across all tested conditions at both 24 and 72 hours, confirming that none of the coatings induced cytotoxic effects. These findings highlight that PMMA, in both its pure form and functionalized with ZnO or ZnO-Ag, does not exhibit harmful effects on hFOB 1.19 cells.

Finally, to assess potential inflammatory or oxidative stress responses induced by the tested materials, nitric oxide (NO) release was measured. NO is a key signaling molecule, and elevated levels are often associated with inflammation and oxidative stress. As shown in Figure 7.12C, NO levels were comparable across the PMMA, PMMA/ZnO, and PMMA/ZnO-Ag coatings at both time points, indicating that the incorporation of ZnO or ZnO-Ag into the composite matrix did not induce pro-inflammatory responses or oxidative stress in hFOB 1.19 cells.

These results support the biocompatibility and safety of the nanostructured coatings, highlighting their potential for use in biomedical applications.

CHAPTER 8. FINAL CONCLUSIONS

The first research direction focused on statistically analyzing the risk factors that lead to post-operative complications associated with dental implants. A rigorous statistical analysis was conducted to assess the influence of factors such as smoking, diabetes, hypertension, compliance with post-operative instructions, and the number of implants on the success rate of implant treatments. The study revealed significant correlations between these factors and the rate of post-operative complications, providing clear guidelines for optimizing therapeutic strategies and improving post-operative monitoring protocols. The results highlighted that patients with a high-risk profile require special attention and personalized monitoring, with adherence to post-operative instructions playing a crucial role in preventing complications.

Beyond the statistical analysis, this research included an experimental approach involving the development and characterization of advanced nanomaterials aimed at improving the performance of dental implants. By integrating innovative nanoparticles, the study demonstrated that the developed materials can significantly enhance interactions with host tissues, contributing to optimized tissue regeneration and the prevention of bacterial biofilm formation. Experimental studies on nanostructured coatings based on PMMA/ZnO(NanoAg) and the use of Zn_2SnO_4@SiO_2 nanoparticles functionalized with 5-FU showed that nanotechnology can significantly contribute to preventing peri-implant infections and optimizing the osseointegration process.

In the second research direction, composite Zn_2SnO_4 nanoparticles coated with SiO_2 and functionalized with 5-Fluorouracil were developed and characterized for bone regeneration and

antimicrobial and antitumor therapy. The SiO_2 layer improved stability in solution and integration into biological matrices, while 5-FU conferred additional antimicrobial and antitumor properties. In vitro studies confirmed high biocompatibility and the ability to support cell proliferation without cytotoxic effects. The nanoparticles also exhibited significant antimicrobial activity against Gram-positive bacteria and bacterial biofilms, highlighting their potential for preventing post-operative infections in maxillofacial reconstruction.

Additionally, an innovative coating based on polymethyl methacrylate (PMMA) enriched with ZnO and ZnO-Ag nanoparticles was developed to protect dental abutments against biofilm formation and peri-implant infections. The nanoparticles were synthesized via a hydrothermal process, achieving uniform morphologies and extended surfaces optimized for antimicrobial interactions. The uniform distribution of nanoparticles within the polymer matrix and their stable adhesion to titanium substrates ensure the coating's efficiency in the oral environment. Microbiological tests demonstrated significant inhibition of biofilm formation and pathogenic agents such as *Staphylococcus aureus*, *Pseudomonas aeruginosa*, and *Candida albicans*. In vitro studies confirmed the biocompatibility of the material, showing no cytotoxic effects on human preosteoblastic cells. This proposed coating has the potential to reduce the risk of peri-implant infections, support tissue regeneration, and improve dental implant integration in modern dental practice.

The integration of statistical results with experimental investigations provides a comprehensive perspective on improving dental implantology, offering a solid foundation for future research aimed at developing personalized and effective solutions for patients requiring oral rehabilitation.

The thesis conclusions emphasize the potential of nanomaterials to prevent biofilm formation and inhibit microbial colonization, two of the most common causes of dental treatment failure. Moreover, the nanoparticles used were proven to be biocompatible and safe in interactions with human cells, paving the way for broader clinical applications.

This research demonstrates that nanotechnology holds the potential to revolutionize modern dentistry, offering innovative solutions for critical issues such as peri-implant infections and bone regeneration. The results support the applicability of nanomaterials in clinical practice and provide a solid foundation for future advancements in smart materials for dental implantology.

However, to fully validate the efficacy and safety of these materials, additional studies in simulated oral environments are necessary, considering factors such as microbial variability, mechanical stress, and the dynamic conditions of the oral cavity. In vivo evaluations will be essential to confirm the in vitro performance and determine the long-term behavior of these materials under the biological and mechanical influences specific to the oral environment.

CHAPTER 9. ORIGINALITY AND INNOVATIVE CONTRIBUTIONS OF THE THESIS

This research has made significant contributions to the field of nanomaterials for dental applications by developing new materials with advanced properties and conducting a rigorous statistical analysis of the risk factors involved in the success of dental implants. The most important original contributions of this study are outlined below:

- A rigorous statistical analysis was performed, enabling the quantification of the impact of various variables and providing an objective basis for optimizing clinical decision-making.

This approach supports the integration of a multidisciplinary strategy aimed at improving dental implantology.

- The study combines expertise in material chemistry, cell biology, and biomedical engineering to propose innovative solutions that overcome the limitations of conventional materials used in dentistry.
- A new type of Zn_2SnO_4 composite nanoparticle coated with SiO_2 and functionalized with 5-Fluorouracil was synthesized, showing high potential for applications in bone regeneration and combined antimicrobial and antitumor therapy.
- A novel coating based on polymethyl methacrylate (PMMA) enriched with ZnO and ZnO-Ag nanoparticles was developed. This coating is designed to protect dental abutments against biofilm formation and peri-implant infections.
- The research has opened new perspectives on the use of nanomaterials for preventing peri-implant infections, optimizing osseointegration, and reducing post-operative complications.
- Through these innovations, the study aims to develop materials capable of reducing the risks associated with peri-implant infections, supporting complex tissue regeneration, and ensuring optimal integration with adjacent tissues. The ultimate goal is to create a solid scientific foundation for introducing nanomaterials into modern dental practice, offering personalized and effective solutions for current clinical needs.

This work has demonstrated that the use of nanotechnology in dentistry has the potential to revolutionize existing treatments, offering innovative solutions to critical issues such as post-implant infections, bone regeneration, and the bioactivity of implants. The original contributions of this study support the clinical applicability of nanomaterials and provide a solid foundation for future research and development in the field of dental implantology.

References

1. Malik, S.; Muhammad, K.; Waheed, Y. Nanotechnology: A Revolution in Modern Industry. *Molecules* **2023**, *28*, doi:10.3390/molecules28020661.
2. Haleem, A.; Javaid, M.; Singh, R.P.; Rab, S.; Suman, R. Applications of nanotechnology in medical field: a brief review. *Global Health Journal* **2023**, *7*, 70-77, doi:https://doi.org/10.1016/j.glohj.2023.02.008.
3. Khan, Y.; Sadia, H.; Ali Shah, S.Z.; Khan, M.N.; Shah, A.A.; Ullah, N.; Ullah, M.F.; Bibi, H.; Bafakeeh, O.T.; Khedher, N.B.; et al. Classification, Synthetic, and Characterization Approaches to Nanoparticles, and Their Applications in Various Fields of Nanotechnology: A Review. *Catalysts* **2022**, *12*, doi:10.3390/catal12111386.
4. Saleh, T.A. Nanomaterials: Classification, properties, and environmental toxicities. *Environmental Technology & Innovation* **2020**, *20*, 101067, doi:https://doi.org/10.1016/j.eti.2020.101067.
5. Altammar, K.A. A review on nanoparticles: characteristics, synthesis, applications, and challenges. **2023**, *14*, doi:10.3389/fmicb.2023.1155622.
6. Abou Neel, E.A.; Bozec, L.; Perez, R.A.; Kim, H.-W.; Knowles, J.C. Nanotechnology in dentistry: prevention, diagnosis, and therapy. *International Journal of Nanomedicine* **2015**, *10*, 6371-6394, doi:10.2147/IJN.S86033.
7. Malik, S.; Muhammad, K.; Waheed, Y. Emerging Applications of Nanotechnology in Healthcare and Medicine. *Molecules* **2023**, *28*, doi:10.3390/molecules28186624.
8. Jandt, K.D.; Watts, D.C. Nanotechnology in dentistry: Present and future perspectives on dental nanomaterials. *Dental Materials* **2020**, *36*, 1365-1378, doi:https://doi.org/10.1016/j.dental.2020.08.006.
9. Nikolova, M.; Slavchov, R.; Nikolova, G. Nanotechnology in Medicine. In *Drug Discovery and Evaluation: Methods in Clinical Pharmacology*, Hock, F.J., Gralinski, M.R., Eds.; Springer International Publishing: Cham, 2020; pp. 533-546.

10. Soliman, S. Nanomedicne: Advantages and Disadvantages of Nanomedicine. *Journal of Nanomedicine & Nanotechnology* **2023**, *14*, doi:10.35248/2157-7439.23.14.666.
11. Moraes, G.; Zambom, C.; Siqueira, W.L. Nanoparticles in Dentistry: A Comprehensive Review. *Pharmaceuticals (Basel, Switzerland)* **2021**, *14*, doi:10.3390/ph14080752.
12. Dakhale, R.; Paul, P.; Achanta, A.; Ahuja, K.P.; Meshram, M. Nanotechnology Innovations Transforming Oral Health Care and Dentistry: A Review. *Cureus* **2023**, *15*, e46423, doi:10.7759/cureus.46423.
13. AlKahtani, R.N. The implications and applications of nanotechnology in dentistry: A review. *The Saudi Dental Journal* **2018**, *30*, 107-116, doi:https://doi.org/10.1016/j.sdentj.2018.01.002.
14. Glowacka-Sobotta, A.; Ziental, D.; Czarczynska-Goslinska, B.; Michalak, M.; Wysocki, M.; Güzel, E.; Sobotta, L. Nanotechnology for Dentistry: Prospects and Applications. *Nanomaterials* **2023**, *13*, doi:10.3390/nano13142130.
15. Umapathy, V.R.; Natarajan, P.M.; SumathiJones, C.; Swamikannu, B.; Johnson, W.M.S.; Alagarsamy, V.; Milon, A.R. Current trends and future perspectives on dental nanomaterials – An overview of nanotechnology strategies in dentistry. *Journal of King Saud University - Science* **2022**, *34*, 102231, doi:https://doi.org/10.1016/j.jksus.2022.102231.
16. Priyadarsini, S.; Mukherjee, S.; Mishra, M. Nanoparticles used in dentistry: A review. *Journal of oral biology and craniofacial research* **2018**, *8*, 58-67, doi:10.1016/j.jobcr.2017.12.004.
17. Niavol, S.S.; Khatibani, A.B.; Hashemi Karouei, S.F.; Hejazi Juybari, S.A.; Moghaddam, H.M. Mesoporous Zn2SnO4 for efficient sensing of ethylene glycol vapor. *Materials Chemistry and Physics* **2023**, *303*, 127799, doi:https://doi.org/10.1016/j.matchemphys.2023.127799.
18. Silvestri, S.; Stefanello, N.; da Silveira Salla, J.; Foletto, E.L. Photocatalytic properties of Zn2SnO4 powders prepared by different modified hydrothermal routes. *Research on Chemical Intermediates* **2019**, *45*, 4299-4313, doi:10.1007/s11164-019-03832-1.
19. E, A.K.N.; S, D.; A, R.; V, N.; A, S. A comparative study of 5-Fluorouracil release from chitosan/silver and chitosan/silver/MWCNT nanocomposites and their cytotoxicity towards MCF-7. *Mater Sci Eng C Mater Biol Appl* **2016**, *66*, 244-250, doi:10.1016/j.msec.2016.04.080.
20. Eshghi Esfahani, R.; Zahedi, P.; Zarghami, R. 5-Fluorouracil-loaded poly(vinyl alcohol)/chitosan blend nanofibers: morphology, drug release and cell culture studies. *Iranian Polymer Journal* **2020**, *30*, 3, doi:10.1007/s13726-020-00882-w.
21. Pandimurugan, A.R.; Sankaranarayanan, K. Antibacterial and photocatalytic activity of ZnO, SnO2 and Zn2SnO4 nanoparticles prepared by Microwave assisted method. *Materials Technology* **2022**, *37*, 717-727, doi:10.1080/10667857.2021.1873635.
22. Anjum, S.; Hashim, M.; Malik, S.A.; Khan, M.; Lorenzo, J.M.; Abbasi, B.H.; Hano, C. Recent Advances in Zinc Oxide Nanoparticles (ZnO NPs) for Cancer Diagnosis, Target Drug Delivery, and Treatment. *Cancers (Basel)* **2021**, *13*, doi:10.3390/cancers13184570.
23. Lakshmi, Y.V.B.; Swapna, P.; Babu, B.K.; Rao, Y.S. Morphology and Anti-microbial Studies of Zinc Stannate Nanoparticles Constructed via Green Synthesis Approach. *Letters in Applied NanoBioScience* **2023**, *12*, doi:10.33263/LIANBS124.138.
24. Dillip, G.R.; Nagajyothi, P.C.; Ramaraghavulu, R.; Banerjee, A.N.; Reddy, B.V.; Joo, S.W. Synthesis of crystalline zinc hydroxystannate and its thermally driven amorphization and recrystallization into zinc orthostannate and their phase-dependent cytotoxicity evaluation. *Materials Chemistry and Physics* **2020**, *248*, 122946, doi:https://doi.org/10.1016/j.matchemphys.2020.122946.
25. Zuo, J.; Quan, Y.; Li, J.; Li, Y.; Song, D.; Li, X.; Wang, Y.; Yi, L.; Wang, Y. Tackling Antibiotic Resistance: Exploring 5-Fluorouracil as a Promising Antimicrobial Strategy for the Treatment of Streptococcus suis Infection. *Animals* **2024**, *14*, 1286.
26. Anzellini, S.; Diaz-Anichtchenko, D.; Sanchez-Martin, J.; Turnbull, R.; Radescu, S.; Mujica, A.; Muñoz, A.; Ferrari, S.; Pampillo, L.; Bilovol, V.; et al. High-Pressure Behavior of Ca2SnO4, Sr2SnO4, and Zn2SnO4. *The Journal of Physical Chemistry C* **2024**, *128*, 1357-1367, doi:10.1021/acs.jpcc.3c06726.
27. Zhang, M.; Song, H.; Yang, S.; Zhang, Y.; Tian, Y.; Wang, Y.; Liu, D. Deciphering the Antibacterial Mechanisms of 5-Fluorouracil in Escherichia coli through Biochemical and Transcriptomic Analyses. *Antibiotics (Basel)* **2024**, *13*, doi:10.3390/antibiotics13060528.
28. Song, W.; Ge, S. Application of Antimicrobial Nanoparticles in Dentistry. *Molecules* **2019**, *24*, 1033.
29. Guerrero Correa, M.; Martínez, F.B.; Vidal, C.P.; Streitt, C.; Escrig, J.; de Dicastillo, C.L. Antimicrobial metal-based nanoparticles: a review on their synthesis, types and antimicrobial action. *Beilstein J Nanotechnol* **2020**, *11*, 1450-1469, doi:10.3762/bjnano.11.129.

30. Rosli, N.A.; Teow, Y.H.; Mahmoudi, E. Current approaches for the exploration of antimicrobial activities of nanoparticles. *Science and Technology of Advanced Materials* **2021**, *22*, 885-907, doi:10.1080/14686996.2021.1978801.
31. Bapat, R.A.; Joshi, C.P.; Bapat, P.; Chaubal, T.V.; Pandurangappa, R.; Jnanendrappa, N.; Gorain, B.; Khurana, S.; Kesharwani, P. The use of nanoparticles as biomaterials in dentistry. *Drug Discovery Today* **2019**, *24*, 85-98, doi:https://doi.org/10.1016/j.drudis.2018.08.012.